

1 **Preservation of Earth-forming events in the W isotopic composition of modern flood basalts**

2

3 **Authors:** Hanika Rizo^{1*}, Richard J. Walker², Richard W. Carlson³, Mary F. Horan³, Sujoy
4 Mukhopadhyay⁴, Vicky Manthos⁴, Don Francis⁵, Matthew G. Jackson⁶

5

6 **Affiliations:**

7 ¹Geotop, Departement des sciences de la Terre et de l'atmosphère, UQAM, Montreal, Canada

8 ²Department of Geology, University of Maryland, College Park, MD, USA ³Carnegie Institution

9 for Science, Washington DC, USA ⁴Department of Earth and Planetary Sciences, UC Davis,

10 Davis, CA, USA ⁵Earth and Planetary Sciences department, McGill University, Montreal, Canada

11 ⁶ Department of Earth Science, UC Santa Barbara, Santa Barbara, CA, USA

12

13 *Corresponding author. E-mail: rizo.hanika@uqam.ca

14

15 **Abstract:** How much of Earth's compositional variation dates to processes occurring during

16 planet formation remains an unanswered question. High precision W isotopic data for rocks from

17 two large igneous provinces, the North Atlantic Igneous Province and the Ontong Java Plateau,

18 reveal preservation to the Phanerozoic of W isotopic heterogeneities in the mantle. These

19 heterogeneities, caused by the decay of ¹⁸²Hf in high Hf/W ratio mantle domains, were created

20 during the first ~50 Ma of Solar System history, and imply that portions of the mantle that

21 formed during Earth's primary accretionary period have survived to the present.

22

23

24 **Main text:**

25 Four and a half billion years of geologic activity has overprinted much of the evidence for
26 processes involved in Earth's formation and initial chemical differentiation. High-precision
27 isotopic measurements, however, now allow the use of the variety of short-lived radionuclides
28 that were present when Earth formed to provide a clearer view of events occurring during the first
29 tens to hundreds of million years (Ma) of Earth history. Evidence from both the ^{146}Sm - ^{142}Nd ($t_{1/2}$
30 = 103 Ma) and ^{129}I - ^{129}Xe ($t_{1/2} = 15.7$ Ma) systems show the importance of early mantle
31 differentiation and outgassing events, but provide conflicting evidence on the preservation of
32 early-formed mantle reservoirs to the present day (1-4). Of these short-lived systems, the ^{182}Hf -
33 ^{182}W ($t_{1/2} = 8.9$ Ma) system is uniquely sensitive to metal-silicate separation, and has been used
34 effectively to trace the timing and processes of core formation (e.g. 5), arguably the most
35 important chemical differentiation event to occur on a rocky planet. Only recently, however, have
36 measurement techniques improved to the point of resolving $^{182}\text{W}/^{184}\text{W}$ variability in ancient (>2.7
37 Ga) terrestrial rocks, that reflects preservation of compositionally distinct domains in Earth's
38 interior that were likely created during Earth formation (6-10). Young mantle-derived rocks
39 examined to date have shown neither ^{142}Nd nor ^{182}W isotopic heterogeneity, suggesting that the
40 early-formed compositional domains in Earth's interior were largely destroyed by mantle mixing
41 processes acting during the first half of Earth history (1-4, 6-10). Here we report $^{182}\text{W}/^{184}\text{W}$ ratios
42 in Phanerozoic flood basalts from Baffin Bay and the Ontong Java Plateau, some of which range
43 to the highest ever measured in terrestrial rocks. These results document the preservation of
44 regions within Earth's interior whose compositions were established by events occurring within
45 the first ~ 50 Ma of Solar System history. This study, consequently, provides new insights into

46 the processes at work during planet formation, the chemical structure of Earth's interior, and the
47 interior dynamics that allowed preservation of chemical heterogeneities for 4.5 billion years.

48
49 Flood basalts are the largest volcanic eruptions identified in the geological record. These types of
50 eruptions created both the North Atlantic Igneous Province, which hosts the Baffin Bay locale
51 (11), and the Ontong Java Plateau, western Pacific Ocean (12). We have studied pillow lavas
52 with high MgO, picritic compositions (Tab. S1) from Padloping Island, Baffin Bay (Pi-23 and
53 Pd-2). We targeted these rocks because some Baffin Bay lavas contain the highest $^3\text{He}/^4\text{He}$ ratios
54 ever measured (e.g. 13), along with Pb isotopic compositions (14) and D/H ratios (15) that
55 indicate that their mantle source was relatively primitive and undegassed, consistent with
56 isolation since shortly after Earth formation. Ontong Java is Earth's largest known volcanic
57 province, and shares chemical and isotopic similarities with the Baffin Bay lavas, consistent with
58 a primitive mantle source (16). The Ontong Java sample (192-1187A-009R-04R) is a basalt
59 (Table S1) collected from the plateau's eastern flank by Ocean Drilling Project Leg 192.

60
61 We present data from the short-lived ^{182}Hf - ^{182}W and ^{146}Sm - ^{142}Nd systems because these two
62 systems are variably sensitive to the core formation and mantle differentiation processes that
63 occurred early in Earth history. We compare these data with data from the long-lived U-Th-He,
64 ^{147}Sm - ^{143}Nd and ^{187}Re - ^{187}Os isotope systems, together with W and highly siderophile element
65 (HSE: Re, Os, Ir, Ru, Pt, Pd) concentrations, to better discern early differentiation events from
66 those occurring over all of Earth history. Glassy rim and core pieces of sample Pi-23 (Pi-23a and
67 Pi-23b, respectively), a bulk sample of Pd-2, and a bulk sample of 192-1187A-009R-04R are
68 characterized by high $^{182}\text{W}/^{184}\text{W}$ ratios that are well resolved from standards, with $\mu^{182}\text{W}$ values

69 ranging from +10 to +48 (where $\mu^{182}\text{W} = [({}^{182}\text{W}/{}^{184}\text{W})_{\text{sample}}/({}^{182}\text{W}/{}^{184}\text{W})_{\text{standard}} - 1] \times 10^6$) (Fig. 1
70 and Table 1, ref. 17). The $\mu^{182}\text{W}$ values for sample Pi-23a and Pi-23b are in good agreement. This
71 rules out the role of stable W isotope fractionation through interaction of seawater with the pillow
72 rim in creating the measured ${}^{182}\text{W}$ values (17). Samples 192-1187A-009R-04R and Pd-2 are
73 characterized by the lowest W concentrations and the highest $\mu^{182}\text{W}$ values (Table 1). The W
74 concentrations of these two samples (23 and 26 ppb, respectively) are broadly consistent with
75 magmas derived by 15-20% partial melting of a mantle source with ~ 5 ppb W, consistent with a
76 primitive source free of W-rich recycled crust (17, Fig. S2). The geological reference materials
77 VE-32 (mid-ocean ridge glass) and BHVO-1 (Hawaiian basalt) were measured at the same time
78 as the Baffin Bay and Ontong Java samples, and yielded $\mu^{182}\text{W}$ values of -0.8 ± 4.5 and $-2.3 \pm$
79 7.7 , respectively (Table 1). These $\mu^{182}\text{W}$ values are indistinguishable from the terrestrial *Alfa*
80 *Aesar* W standard ($\mu^{182}\text{W} = 0$) and other modern rocks (6-10). The ${}^3\text{He}/{}^4\text{He}$ ratio measured in
81 olivines of the Baffin Bay samples (Table S3, 17) yielded values up to 48.4 R_A (R_A being the
82 ${}^3\text{He}/{}^4\text{He}$ ratio normalized to the atmospheric ratio of 1.39×10^{-6}) which are in agreement of
83 previous findings (13) and indicate that the source of these lavas is relatively undegassed, and
84 possibly isolated since Earth formation. The Baffin Bay and Ontong Java Plateau samples have
85 HSE abundances and initial ${}^{187}\text{Os}/{}^{188}\text{Os}$ ratios (providing a record of long-term Re/Os ratio) that
86 are indistinguishable from other modern mantle-derived lavas with similar MgO abundances that
87 do not show elevated $\mu^{182}\text{W}$ (Figure 2, Table S4, 18).

88
89 Variability in ${}^{182}\text{W}/{}^{184}\text{W}$ ratios reflects Hf/W fractionation while ${}^{182}\text{Hf}$ was extant. Fractionations
90 in Hf/W are observed in early Solar System materials (e.g. 5), so variable tungsten isotopic
91 compositions in terrestrial samples can reflect the imperfect mixing of late additions of such

92 materials (6, 9). The $\mu^{182}\text{W}$ value of +48 for Baffin Bay sample Pd-2, however, is larger than can
93 be accounted for by this process, and so this possibility is discounted (see Supplementary Text).
94 Fractionation of Hf/W can also have occurred as the result of endogenous Earth differentiation
95 processes such as magma ocean crystallization (7) and core formation (9). Silicate fractionation
96 processes, however, cannot be responsible for the generation of the anomalous ^{182}W in the
97 sources of Baffin Bay and Ontong Java lavas. If the high $\mu^{182}\text{W}$ was due to silicate fractionation
98 in a magma ocean while ^{182}Hf was extant, then $\mu^{182}\text{W}$ should positively correlate with $\mu^{142}\text{Nd}$, the
99 decay product of the short-lived ^{146}Sm ($t_{1/2} = 103$ Ma) isotope system. Instead, the $\mu^{142}\text{Nd}$ values of
100 the samples are indistinguishable from all other modern basalts so far measured (Fig. S3, Table
101 S5, 17).

102
103 This leaves fractionation of Hf/W as a result of metal-silicate segregation accompanying core
104 formation as the probable cause of the observed anomalies in the Phanerozoic samples. Metal-
105 silicate segregation is the most effective process capable of fractionating Hf/W ratios, because Hf
106 is a strongly lithophile trace element, while W is moderately siderophile. The low W
107 concentrations estimated for the mantle source of the flood basalts studied here are consistent
108 with mantle domains that experienced metal-silicate segregation (Table 1, Supplementary Text).
109 Repeated metal-silicate segregation events during planet formation (19) could create one or more
110 mantle domains with distinct $\mu^{182}\text{W}$ without affecting the Sm-Nd system. Such events would
111 result in variable $\mu^{182}\text{W}$ due to different times of the metal-silicate segregation events (Figure 3),
112 or different Hf/W ratios in the resulting mantle reservoirs that reflect differing oxidation states,
113 and hence, differing W partitioning into metal (Supplementary Text). The key observation, which
114 is also seen in the results reported here, is that terrestrial samples with ^{182}W excesses do not seem

115 to derive from sources depleted in HSE (Figure 2, 6-10). Highly siderophile elements have
116 partition coefficients between metal and silicate of $>10^4$ (20), thus, their concentrations in metal-
117 depleted mantle domains are expected to be very low. Evolving oxidation states during Earth
118 accretion might explain the decoupling of ^{182}W and HSE, because while W becomes less
119 siderophile under oxidizing conditions, the HSE, even at high oxidation states, are not soluble in
120 silicates (20). This type of model, however, requires subsequent late accreted HSE to be mixed
121 into different mantle domains without the mixing away of tungsten isotopic heterogeneity.
122 Alternatively, the observed decoupling could be explained if some metal from the core of the
123 Moon-forming giant impactor was retained in the mantle, followed by a minor amount of late
124 accretion (9). This type of model requires that a substantial mass of high density metal be
125 retained in the Earth' mantle following the impact, when the mantle was partially or wholly
126 molten, and that the retained metal contained chondritic relative abundances of the HSE. These
127 models and others have been presented to try to explain the apparent decoupling of W isotopic
128 compositions and HSE abundance variations. These models are summarized in the
129 Supplementary Text along with a few additional suggestions.

130
131 Regardless of the origin of the ^{182}W variability, arguably more surprising than the fact that Earth
132 experienced such early differentiation events, is that reservoirs formed by these early processes
133 remain in the mantle today. This conclusion is now supported by data from both W and Xe (1,
134 22) isotopic variability, but not ^{142}Nd , where the evidence suggests that the observed
135 heterogeneity in $^{142}\text{Nd}/^{144}\text{Nd}$ ratio was reduced to an unobservable level by the end of the
136 Archean, likely though the mixing caused by mantle convection. Perhaps a key to reconcile these
137 observations is that the ^{129}I - ^{129}Xe system primarily reflects mantle outgassing, and the ^{182}Hf - ^{182}W

138 system metal-silicate separation, whereas the ^{146}Sm - ^{142}Nd system is controlled by internal mantle
139 differentiation. For both W and Xe, one component of the complementary chemical
140 differentiation, the core for W, and the atmosphere for Xe, may not be available for effective
141 recycling and mixing in the mantle (23). By contrast, for Nd, the main reservoirs created during
142 early Earth differentiation may have been in a portion of the mantle that has been effectively
143 mixed by mantle circulation. Estimates for how much of the mantle can remain unmixed depend
144 on the rheological properties assigned to the various materials involved. Some models (e.g. 24)
145 show that as much as 20% of the mantle may remain isolated as distributed masses in the mantle.
146 An important aspect of the results presented here is that both ^{182}W anomalies and elevated
147 $^3\text{He}/^4\text{He}$ (Table S3) appear in at least two major flood basalts. These events produce huge
148 volumes of magma that must be derived by melting large volumes of mantle during unusual
149 thermal events in the history of mantle circulation. The large size and sporadic nature of flood
150 basalts is perhaps more indicative of a layer in the mantle that has an appropriate density or
151 rheological properties to keep it from effectively mixing with the rest of the mantle. One
152 candidate for such a reservoir is the large low seismic shear velocity provinces (LLSVP) imaged
153 at the base of the mantle (25). These regions appear to be warmer and compositionally different
154 from surrounding mantle. Estimates of their volume range to as high as 7% of the mantle, or of
155 order $6 \times 10^{10} \text{ km}^3$. If the LLSVP are remnants of early differentiation events on Earth, they must
156 have a delicately balanced density contrast compared to the surrounding mantle to allow their
157 survival through 4.5 billion years of dynamic Earth history.

158

159 **References and notes:**

- 160 1. S. Mukhopadhyay, Early differentiation and volatile accretion recorded in deep-mantle neon
161 and xenon. *Nature* **486**, 101-104 (2012).
- 162 2. M. Boyet, M. O. Garcia, R. Pik, F. Albarede, A search for ^{142}Nd evidence of primordial mantle
163 heterogeneities in plume basalts. *Geophys. Res. Lett.* **32**, no. 4 (2005).
- 164 3. V.C. Bennett, A.D. Brandon, A.P. Nutman, Coupled ^{142}Nd - ^{143}Nd isotopic evidence for Hadean
165 mantle dynamics, *Science* **318**, 1907-1910 (2007).
- 166 4. H. Rizo, M. Boyet, J. Blichert-Toft, M.T. Rosing, Early mantle dynamics inferred from ^{142}Nd
167 variations in Archean rocks from southwest Greenland, *Earth Planet. Sci. Lett.* **377**, 324-355
168 (2013).
- 169 5. T. Kleine, M. *et al.*, Hf–W chronology of the accretion and early evolution of asteroids and
170 terrestrial planets. *Geochim. Cosmochim. Acta* **73**, 5150-5188 (2009).
- 171 6. M. Willbold, T. Elliott, S. Moorbath, The tungsten isotopic composition of the Earth's mantle
172 before the terminal bombardment. *Nature* **477**, 195-198 (2011).
- 173 7. M. Touboul, I.S. Puchtel, R.J. Walker, ^{182}W evidence for long-term preservation of early
174 mantle differentiation products. *Science* **335**, 1065-1069 (2012).
- 175 8. M. Touboul, J. Liu, J. O'Neil, I.S. Puchtel, R.J. Walker, New insights into the Hadean mantle
176 revealed by ^{182}W and highly siderophile element abundances of supracrustal rocks from the
177 Nuvvuagittuq Greenstone Belt, Quebec, Canada. *Chem. Geol.* **383**, 63-75 (2014).
- 178 9. M. Willbold, S.J. Mojzsis, H.-W. Chen, T. Elliot, Tungsten isotope composition of the Acasta
179 Gneiss Complex. *Earth Planet. Sci. Lett.* **419**, 168-177 (2015).
- 180 10. H. Rizo *et al.*, Early Earth differentiation investigated through ^{142}Nd , ^{182}W , and highly
181 siderophile element abundances in samples from Isua, Greenland, *Geochim. Cosmochim. Acta*
182 **175**, 319-336 (2016).

- 183 11. A.D. Saunders, J.G. Fitton, A.C. Kerr, M.J. Norry, R.W. Kent, The North Atlantic igneous
184 province. *Geophys. Mon. Series* **100**, 45-94 (1997).
- 185 12. C.R. Neal, J.J. Mahoney, L.W. Kroenke, R.A. Duncan, M.G. Petterson, The Ontong Java
186 Plateau. *Geophys. Mon. Series* **100**, 183-216 (1997).
- 187 13. N.A. Starkey et al., Helium isotopes in early Iceland plume picrites: Constraints on the
188 composition of high $^3\text{He}/^4\text{He}$ mantle. *Earth Planet. Sci. Lett.* **277**, 91-100 (2009).
- 189 14. M.G. Jackson *et al.*, Evidence for the survival of the oldest terrestrial mantle reservoir. *Nature*
190 **466**, 853-856 (2010).
- 191 15. L. J. Hallis *et al.*, Evidence for primordial water in Earth's deep mantle. *Science* **350**, 795-797
192 (2015).
- 193 16. M.G. Jackson, R.W. Carlson, An ancient recipe for flood-basalt genesis. *Nature* **476**, 316-319
194 (2011).
- 195 17. Materials and Methods are available as Supplementary Materials on *Science* Online
- 196 18. C.W. Dale *et al.*, Osmium isotopes in Baffin Island and West Greenland picrites: implications
197 for the $^{187}\text{Os}/^{188}\text{Os}$ composition of the convecting mantle and the nature of high $^3\text{He}/^4\text{He}$ mantle.
198 *Earth Planet. Sci. Lett.* **278**, 267-277 (2009).
- 199 19. D. Rubie, F. Nimmo, H.J. Melosh, Formation of Earth's core. *Treatise on Geophysics*,
200 Second Edition, 2015.
- 201 20. H. St. C. O'Neill *et al.*, Experimental petrochemistry of some highly siderophile elements at
202 high temperatures, and some implications for core formation and the mantle's early history. *Chem.*
203 *Geol.* **120**, 255-273 (1995).

- 204 21. J. M. D. Day *et al.*, Origin of felsic achondrites Graves Nunataks 06128 and 06129, and
205 ultramafic brachinites and brachinite-like achondrites by partial melting of volatile-rich primitive
206 parent bodies. *Geochim. Cosmochim. Acta*, **81**, 94-128 (2012).
- 207 22. M.K. Pető, S. Mukhopadhyay, K.A. Kelley, Heterogeneities from the first 100 million years
208 recorded in deep mantle noble gases from the Northern Lau Back-arc Basin. *Earth Planet. Sci.*
209 *Lett.* **369**, 13-23 (2013).
- 210 23. M.G. Jackson *et al.*, Peridotite xenoliths from the Polynesian Austral and Samoa hotspots:
211 Implications for the destruction of ancient ^{187}Os and ^{142}Nd isotopic domains and the preservation
212 of Hadean ^{129}Xe in the modern convecting mantle. *Geochim. Cosmochim. In press* (2016).
- 213 24. J.P. Brandenburg, E.H. Hauri, P.E. van Keken, C.J. Ballentine, A multiple-system study of
214 the geochemical evolution of the mantle with force-balanced plates and thermochemical effects.
215 *Earth Planet. Sci. Lett.* **376**, 1-13 (2008).
- 216 25. E.J. Garnero, A.K. McNamara, Structure and dynamics of Earth's lower mantle, *Science* 320,
217 626-628 (2008)
- 218 26. M. Horan *et al.*, Highly siderophile elements in chondrites. *Chem. Geol.* **196**, 5-20 (2003).
- 219 27. T. J. Ireland, R.J. Walker, M.O. Garcia, Highly siderophile element and ^{187}Os isotope
220 systematics of Hawaiian picrites: implications for parental melt composition and source
221 heterogeneity, *Chem. Geol.* **260**, 112-128 (2009).
- 222 28. W. B. Tonks and H. J. Melosh, Magma ocean formation due to giant impacts, *J. Geophys.*
223 *Res. : Planets* 98, **E3**, 5319-5333 (1993).
- 224 29. F. R. Boyd, S.A. Mertzman, Magmatic processes: Physicochemical principles, 13-24 (1987).
- 225 30. M. Touboul, R. J. Walker, High precision tungsten isotope measurement by thermal
226 ionization mass spectrometry. *Int. J. Mass Spectrom.* **309**, 109 (2011).

- 227 31. E. Gayer, S. Mukhopadhyay, B.J. Meade, *Earth Planet. Sci. Lett.* **266**, 303-315 (2008).
- 228 32. A.S. Cohen, F.G. Waters, Separation of osmium from geological materials by solvent
229 extraction for analysis by thermal ionisation mass spectrometry. *Anal. Chim. Acta* **332**, 269-275
230 (1996).
- 231 33. J.L. Birck, M. Roy-Barman, F. Capman, Re-Os isotopic measurements at the femtomole level
232 in natural samples. *Geostandards Newsletter* **20**, 19-27 (1997).
- 233 34. M. Rehkämper, A.N. Halliday, Accuracy and long-term reproducibility of lead isotopic
234 measurements by MC-ICP-MS using an external method for correction of mass discrimination.
235 *Int. J. Mass Spectrom.* **181**, 123-133 (1998).
- 236 35. I.S. Puchtel, *et al*, Insights into early Earth from the Pt–Re–Os isotope and highly siderophile
237 element abundance systematics of Barberton komatiites. *Geochim. Cosmochim. Acta* **125**, 394-
238 413 (2014).
- 239 36. M. Boyet, R.W. Carlson, ¹⁴²Nd evidence for early (> 4.53 Ga) global differentiation of the
240 silicate Earth. *Science* **309**, 576-581 (2005).
- 241 37. H. Tazoe, H. Obata, T. Gamo, Determination of cerium isotope ratios in geochemical samples
242 using oxidative extraction technique with chelating resin. *J. Analytical Atomic. Spectroscopy* **22**,
243 616-622 (2006).
- 244 38. Hirahara Y. *et al.*, Detailed bathymetric features in the outer-arc high off the northwest
245 Sumatra-results from KY09-09 cruise. *JAMSTEC Rep. Res. Dev.* **15**, 27-33 (2012).
- 246 39. R.W. Carlson, M. Boyet, M. Horan, Chondrite barium, neodymium, and samarium isotopic
247 heterogeneity and early earth differentiation. *Science* **316**, 1175-1178 (2007).

- 248 40. R.J. Walker, Highly siderophile elements in the Earth, Moon and Mars: update and
249 implications for planetary accretion and differentiation. *Chem. Erde-Geochem.* **69**, 101-125
250 (2009).
- 251 41. M.A. Bouhifd *et al.*, Superchondritic Sm/Nd ratio of the Earth: Impact of Earth's core
252 formation. *Earth Planet. Sci. Lett.* **413**, 158-166 (2015).
- 253 42. J. Wade, B.J. Wood, J. Tuff, Metal–silicate partitioning of Mo and W at high pressures and
254 temperatures: evidence for late accretion of sulphur to the Earth. *Geochim. Cosmochim. Acta* **85**,
255 58-74 (2012).
- 256 43. J.M.D. Day *et al.*, Late accretion as a natural consequence of planetary growth. *Nature*
257 *Geoscience* **5**, 614-617 (2012).
- 258 44. J.H. Jones, M.J. Drake, Geochemical constraints on core formation in the Earth. *Nature* **322**,
259 221-228 (1986).
- 260 45. J. Li and C. B. Agee, Geochemistry of mantle–core differentiation at high pressure. *Nature*
261 **381**, 686-689 (1996).
- 262 46. M.L.G. Tejada *et al.*, Pin-pricking the elephant: Evidence on the origin of the Ontong Java
263 Plateau from Pb-Sr-Hf-Nd isotopic characteristics of ODP Leg 192 basalts. *Geol. Soc. London*
264 *Spec. Publ.* **229**, 133-150 (2004).
- 265 47. Brenan J. M. and McDonough W. F. (2009) Core formation and metal-silicate fractionation
266 of osmium and iridium from gold. *Nature Geosciences*, **2**, 798-801.
- 267 48. Wheeler, K.T., Walker, D., and McDonough, W.F. (2010) Pd and Ag metal-silicate
268 partitioning applied to Earth differentiation and core-mantle exchange. *Meteoritics and Planetary*
269 *Science* **46**, 199-217.

- 270 49. R. Arevalo, W.F. McDonough, Tungsten geochemistry and implications for understanding
271 the Earth's interior. *Earth Planet. Sci. Lett.* **272**, 656-665 (2008).
- 272 50. S. König *et al.*, The Earth's tungsten budget during mantle melting and crust formation.
273 *Geochim. Cosmochim. Acta* **75**, 2119-2136 (2011).
- 274 51. D. Francis. The Baffin Bay lavas and the value of picrites as analogues of primary magmas.
275 *Contrib. Mineral. Petr.* **89**, 144-154 (1985).
- 276 52. A. Corgne *et al.*, Silicate perovskite-melt partitioning of trace elements and geochemical
277 signature of a deep perovskitic reservoir. *Geochim. Cosmochim. Acta* **69**, 485-496 (2005).
- 278 53. K. Righter, C. K. Shearer, Magmatic fractionation of Hf and W: constraints on the timing of
279 core formation and differentiation in the Moon and Mars. *Geochim. Cosmochim. Acta* **67**, 2497-
280 2507 (2003).
- 281 54. M. Boyet, R.W. Carlson, M. Horan, Old Sm-Nd ages for cumulate eucrites and
282 redetermination of the solar system initial $^{146}\text{Sm}/^{144}\text{Sm}$ ratio. *Earth Planet. Sci. Lett.* **291**, 172-181
283 (2010).
- 284 55. C. Vockenhuber *et al.*, ^{182}Hf , a new isotope for AMS. *Nuclear Instruments and Methods in*
285 *Physics Research Section B: Beam Interactions with Materials and Atoms* **223**, 823-828 (2004).
- 286 56. G. Caro, B. Bourdon, Non-chondritic Sm/Nd ratio in the terrestrial planets: consequences for
287 the geochemical evolution of the mantle-crust system. *Geochim. Cosmochim. Acta* **74**, 3333-
288 3349 (2010).

289

290 **Acknowledgments:** We thank T. Mock for assistance with mass spectrometry. This work was
291 improved by helpful discussions with J. O'Neil, S. Shirey and B. Wood. We thank S. Shirey who
292 provided sample VE-32. We also thank the helpful comments and suggestions from three

293 anonymous reviewers and the editor B. Grocholski. We thank M. Garçon who developed the 4-
294 step ^{142}Nd acquisition method. This work was supported by NSF-CSEDI grant EAR1265169 to
295 R.J. Walker, and by EAR1250419 to S. Mukhopadhyay. All data are available in the main
296 manuscript and supplementary materials.

297
298 **Figure 1. $\mu^{182}\text{W}$ values measured for Baffin Bay and Ontong Java Plateau samples, the**
299 **geological reference materials VE-32 and BHVO-1 and the *Alfa Aesar W* standard.** The
300 values are expressed as parts in 10^6 or ppm deviations from the average measured from the W
301 standard. The grey shaded area represents the 2 standard deviation (2σ) for the W standard
302 measurements. Errors for each data point are 2σ .

303
304 **Figure 2. Highly siderophile element abundances (HSE) for the Baffin Bay and Ontong**
305 **Java Plateau samples.** Abundances are normalized to the HSE of carbonaceous chondrites (CI)
306 of ref. 26. Grey shaded area shows the range of HSE abundances for type-2 Hawaiian picrites
307 (ref. 27).

308
309 **Figure 3. Model for the creation of distinct W isotopic mantle reservoirs.** (A) Early core
310 formation leaves the proto-Earth's mantle with a high Hf/W ratio that, with time, evolves to a
311 high $\mu^{182}\text{W}$ value (i). (B) The impact of a large body affects the Hf/W ratio and W isotopic
312 composition of a portion of the proto-Earth's mantle. (C) Evolution of the portion of the mantle
313 (ii) affected by the impact of a large body, involving some degree of isotopic equilibration
314 between impactor materials and mantle. The core of the impactor subsequently merges with the
315 core of the proto-Earth. (D) Possible scenario after isostatic adjustment (e.g. 28), and creation of

316 a mantle with heterogeneous $\mu^{182}\text{W}$ through impacts of large bodies. Mantle domains affected by
 317 impacts that occur after the extinction of ^{182}Hf , will no longer generate radiogenic ^{182}W , so their
 318 $^{182}\text{W}/^{184}\text{W}$ ratios will change only by mixing with other terrestrial reservoirs or with late-accreted
 319 chondritic material. (E) Late accretion representing $\sim 0.5\%$ of Earth's mass decreases the
 320 $^{182}\text{W}/^{184}\text{W}$ ratio of all the earlier formed reservoirs by ~ 15 ppm. This last accretion is responsible
 321 for endowing the modern mantle with chondritic relative abundances of the HSE.

322

Locality	Geodynamic context	Sample	$\mu^{182}\text{W}$ (ppm)	$\pm 2\sigma$ (ppm)	W (ppb)
Baffin Bay	Flood basalt	Pi-23 a	11.9	5.9	62
Baffin Bay	Flood basalt	Pi-23 b	8.3	5.6	62
Baffin Bay	Flood basalt	Pd-2	48.4	4.6	26
Ontong Java Plateau	Flood basalt	192-1187A 009R 04R	23.9	5.3	23
East Pacific Rise	Mid-ocean ridge basalt	VE-32	-0.8	4.5	54
Hawaii	Ocean island basalt	BHVO-1	-2.3	7.7	274

323

324

325 **Table 1.** Tungsten concentrations and isotopic compositions measured for Baffin Bay samples
 326 Pi-23a, Pi-23b, Pd-2, the Ontong Java Plateau sample 192-1187A 009R 04R, the MORB glass
 327 sample VE-32, the BHVO-1 basalt standard. Uncertainties are 2σ . More details are given in ref.
 328 17 and Table S2.

329

330 **Supplementary Materials:**

331 Materials and Methods

332 Figures S1-S7

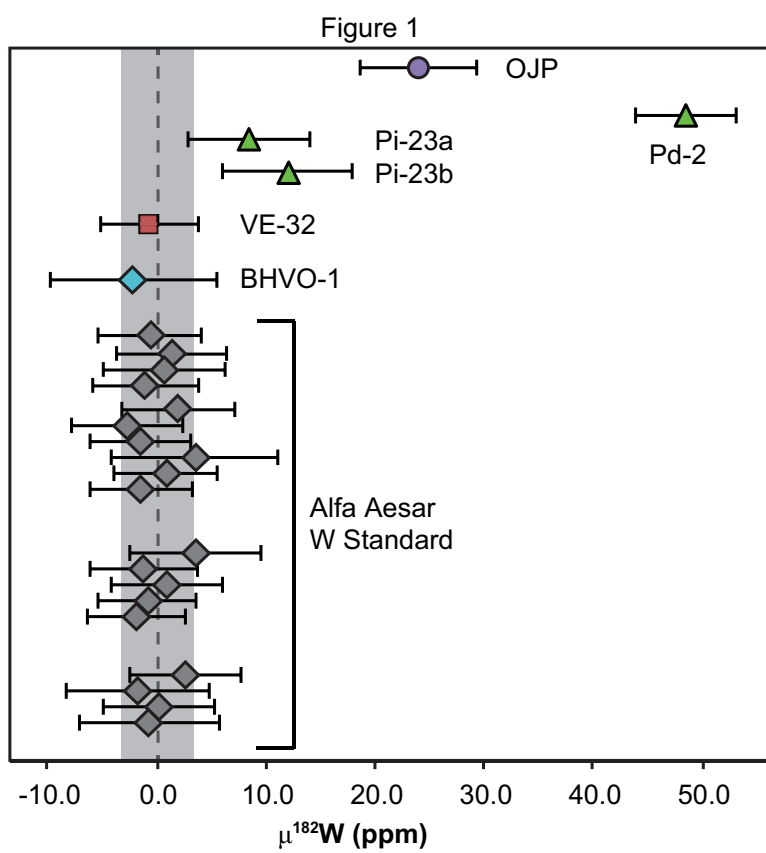
333 Tables S1-S5

334 References (29-56)

335

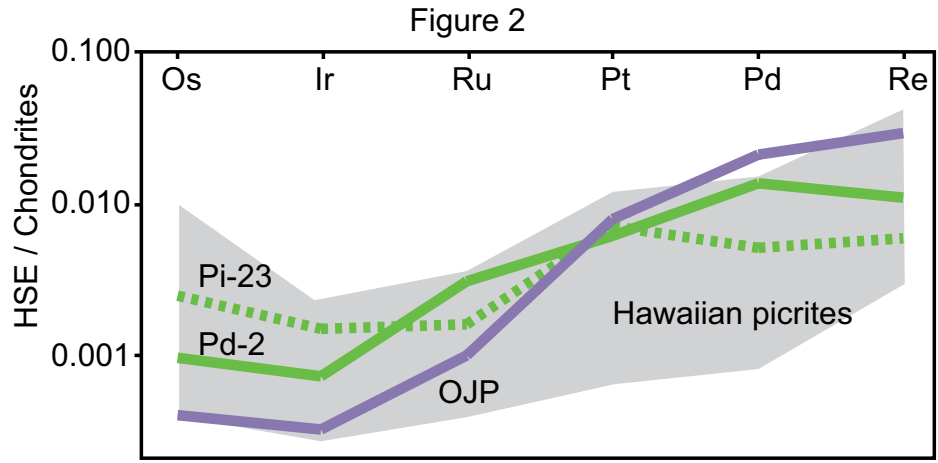
336 **Figures**

337



338

339

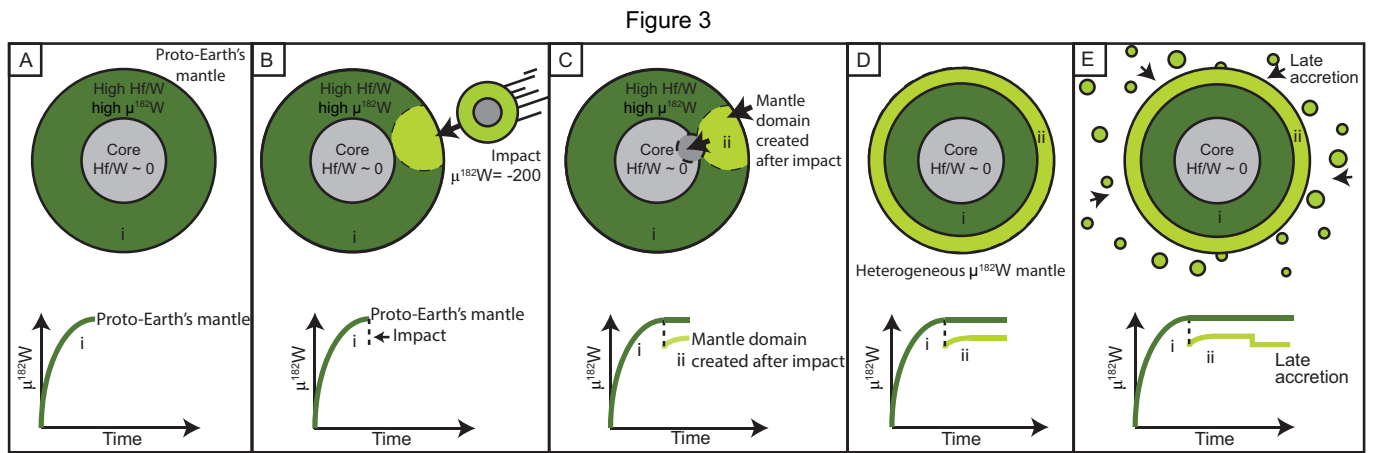


340

341

342

343



344